Heat Balance and Eddies in the Caribbean Upwelling System

JULIEN JOUANNO AND JULIO SHEINBAUM

Departamento de Oceanografía Física, CICESE, Ensenada, Baja California, Mexico

ABSTRACT

The upper-ocean heat budget of the Caribbean upwelling system is investigated during the onset of the Atlantic warm pool (June–September) using high-resolution observations of sea surface temperature and a high-resolution ($1/12°$) regional model. Vertical mixing is found to be the major cooling contribution to the mixed layer heat budget in the nearshore and offshore Colombia Basin. Numerical results show that intense mesoscale eddies in the Colombia Basin significantly shape the turbulent cooling and may participate in the maintenance of cooler temperature in this region compared to surrounding areas. Indeed, increased mixing at the base of the mixed layer occurs below energetic surface jets that form on the downstream side of the eddies. These jets generally flow offshore and may arise from the deformation of the surface mesoscale field. It is shown that significant contribution of horizontal advection to the mixed layer heat budget is limited to a radius of 300 km around the Guajira and Margarita upwelling zones.

1. Introduction

As part of the Atlantic warm pool (AWP; Wang et al. 2006), the Caribbean Sea plays an important role in the regional climate system during boreal summer and fall. The variability of the sea surface temperature (SST) in the region is thought to influence tropical cyclogenesis (Inoue et al. 2002), to modulate the rainfall reaching the Americas (Wang et al. 2006), and to participate in the maintenance of the Caribbean low-level jet (CLLJ; Wang 2007).

A numerical study shows that the warming rate over the Caribbean region during the onset and peak phases (June–October) of the AWP are limited by the southern Caribbean upwelling system (Lee et al. 2007). The presence of cooler waters in the southern Caribbean during this period is illustrated either in snapshots (Fig. 1) or climatological averages (Fig. 2a) of observed SST. The cold waters at the coast are commonly explained by a persistent coastal upwelling forced by the alongshore CLLJ (Inoue et al. 2002; Andrade and Barton 2005; Lee et al. 2007). But away from the coast (>100 km), there is no consensus regarding the mechanism explaining the cool surface conditions. Inoue et al.

(2002) and Andrade and Barton (2005) proposed that offshore cooling could be due to Ekman pumping forced by the intense positive wind stress curl over the southern half of the basin. Lee et al. (2007) suggest that horizontal advection by the Caribbean Current of the cold waters upwelled at the coast may contribute to the maintenance of cool conditions offshore. In a similar way, Andrade and Barton (2005) noticed that upwelling filaments expel cooler and chlorophyll-rich coastal waters westward and northward into the Caribbean Sea.

Energetic eddies are known to dominate the upper-ocean variability in the Caribbean Sea (Fig. 1). Recent results have shown that their energy varies at seasonal and interannual scales in response to variations of the CLLJ, through modulation of the westward Caribbean Current and instability processes (Jouanno et al. 2012). The energy of the eddies is maximum in the Colombia Basin (west of 70°W), with an annual peak between July and October, that is, during the onset of the AWP. Other studies provide some insight into the role played by mesoscale dynamics in eastern boundary upwelling systems. In the California Current system, Marchesiello et al. (2003) find that eddies and filaments mix cold nearshore water with warm offshore water. Colas et al. (2011) report that the offshore cooling in the Peru and Chile upwelling systems (up to 500 km offshore) is sustained by a combination of both mean flow advection and eddy fluxes. Although the mesoscale

Corresponding author address: Julien Jouanno, Departamento de Oceanografía Física, CICESE, Km. 107 Carr Tijuana-Ensenada, Ensenada Baja California 22860, Mexico.
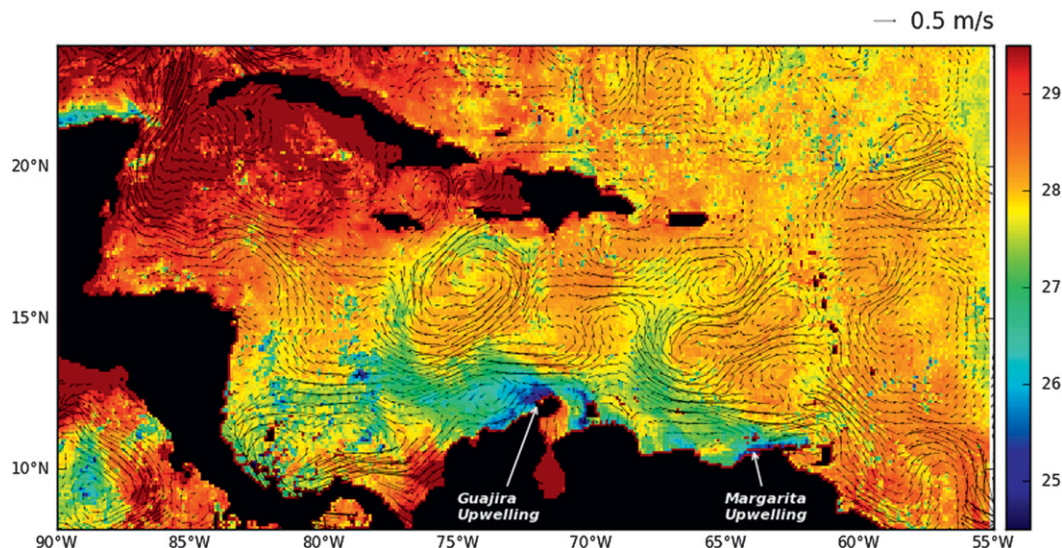E-mail: jouanno@cicese.mx

FIG. 1. Sea surface temperature (°C) and absolute geostrophic surface currents from AVISO on 5 Aug 2009 inferred from satellite observations.

eddies have often been suspected to affect the Caribbean SSTs (Inoue et al. 2002; Andrade and Barton 2005), their role in the regional heat balance has never been investigated.

The aim of this study is to revisit the upper ocean heat budget in the Caribbean Sea during the onset of the AWP, with a special focus on the role played by the mesoscale eddies at this time. The paper is organized as follows. Simulation characteristics and observations are presented in section 2. The heat budget and the mechanisms whereby the eddies modulate the SSTs are analyzed in section 3. Section 4 provides a discussion and summary of the results.

2. Model and data

The regional simulation used in this study is the one analyzed in Jouanno et al. (2012). The numerical code is that of the model Nucleus for European Modeling of the Ocean (NEMO) (Madec 2008). The regional grid of 1/12° horizontal resolution encompasses the Gulf of Mexico and the Caribbean Sea (5°–33°N, 100°–55°W). It has 75 levels in the vertical, with 12 levels in the upper 20 m and 24 levels in the upper 100 m. The model is forced at its lateral boundaries with outputs from the global interannual experiment ORCA025-MJM95 developed by the DRAKKAR team (Barnier et al. 2006). The open boundary conditions radiate perturbations out of the domain and relax the model variables to 5-day averages of the global experiment. Details of the method are given in Tréguier et al. (2001). The vertical turbulent mixing is parameterized using a level-1.5 turbulence

closure scheme (TKE; Blanke and Delecluse 1993). The atmospheric fluxes of momentum, heat, and freshwater are provided by bulk formulae (Large and Yeager 2004) and European Centre for Medium-Range Weather Forecasts (ECMWF) Interim Re-Analysis (ERA-Interim) (3-h fields of wind, atmospheric temperature, and humidity; daily fields of long, shortwave radiation and precipitation). The model is initialized on 31 December 1990 with temperature and salinity outputs from the global experiment at the same date and then integrated over the period 1991–2009. Five-day averages from 2003 to 2009 are analyzed. We refer the reader to Jouanno et al. (2012) for further details on the model configuration. The analysis in Jouanno et al. (2012) shows that the seasonal and interannual variability of the eddy energy and background currents in the model are in good agreement with that inferred from satellite observations. Model SSTs are compared with National Oceanic and Atmospheric Administration (NOAA) CoastWatch blended SST (1/10° resolution).

3. Results

Observations during June–September show that the SSTs in the southern Caribbean Sea are cooler than the surrounding waters (Fig. 2a). In the Colombia Basin, there is a clear contribution of the Guajira upwelling at the coast (12°N, 72°W; Andrade and Barton 2005), but cool conditions also occur west and north, 1000 km away from the upwelling area. The temperature gradients suggest a dynamical connection between the cold waters nearshore and the cooled conditions offshore. In the
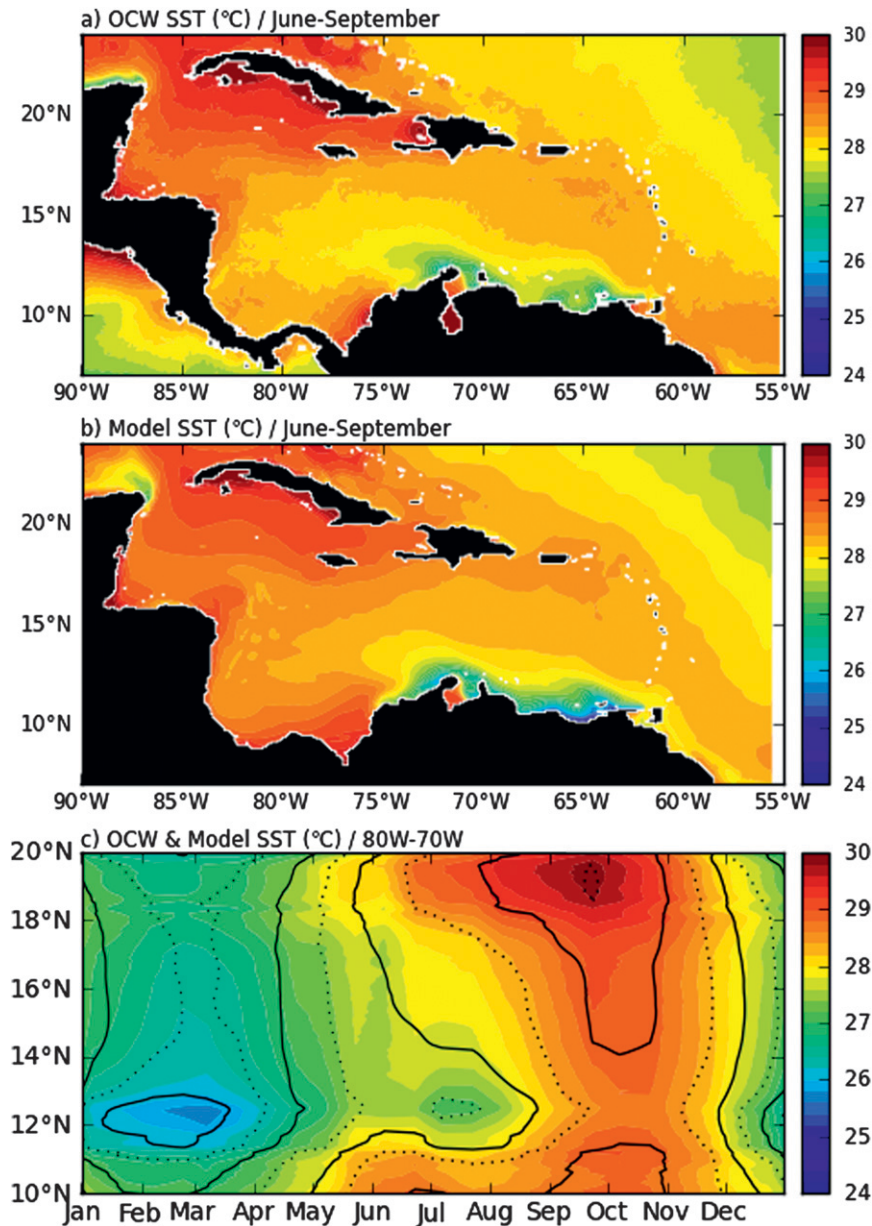
FIG. 2. Mean climatological SST in the Caribbean Sea (°C): horizontal distribution during June–September from (a) observations and (b) model and (c) time–latitude distribution of temperatures averaged between 80° and 70°W, for the model (colors) and satellite observations (contours). Interval between contours is 0.5°C (solid lines for integer values, dotted lines otherwise). The considered period is 2003–09.

Venezuela Basin (east of 70°W), the cool conditions are confined within 300 km of the Margarita upwelling area (10°N, 64°W). In the model (Fig. 2b), the cooled waters in the northwest of the Colombia Basin do not reach as far as in the observations, but the simulation is able to reproduce the cool temperature anomaly in the Colombia Basin, which contrasts with the warm waters located north of Jamaica and in the southern Gulf of

Panama. Latitude–time diagrams of model and observed seasonal SST in the Colombia Basin (average between 80° and 70°W) also illustrate that the warming from June to September is strongly reduced between 11° and 18°N (Fig. 2c). Throughout the year the coolest waters are observed between 12° and 13°N, at the latitude of the Guajira upwelling. There, the meridional contrast of temperature is maximum in

January–March and June–August, indicative that the Guajira upwelling is maximum during these periods, in agreement with the semiannual cycle of the CLLJ (Wang 2007).

To determine the processes driving the distribution of the SSTs, the different contributions to the mixed layer equation are analyzed. The mixed layer temperature equation is computed following Menkes et al. (2006):

$$\partial_t \langle T \rangle = \underbrace{-\langle u \partial_x T \rangle - \langle v \partial_y T \rangle - \langle w \partial_z T \rangle}_{A} + \underbrace{\langle D_l(T) \rangle}_{B} \underbrace{- \frac{1}{h} \frac{\partial h}{\partial t} (\langle T \rangle - T_{z=-h})}_{C} + \underbrace{\frac{Q_{ns} + Q_s(1 - f_{z=-h})}{\rho_0 C_p h}}_{D} + \underbrace{\frac{1}{h}(K_z \partial_z T)_{z=-h}}_{E} ,$$

with

$$\langle \cdot \rangle = \frac{1}{h} \int_{-h}^{0} \cdot \, dz .$$

Here, T is the model potential temperature, (u, v, w) are the velocity components, $D_l(T)$ is the lateral diffusion operator, K_z is the vertical diffusion coefficient for tracers, and h is the mixed layer depth. Here, Q_{ns} and Q_s are the nonsolar and solar components of the air–sea heat flux, and $f_{z=-h}$ is the fraction of the shortwave radiation that reaches the mixed layer depth. The $\langle \cdot \rangle$ represents depth averaged integration over the variable mixed layer depth (MLD). The MLD is defined as the depth where density increase compared to density at 10 m equals 0.03 kg m^{-3}. A represents the advection, B is the lateral diffusion, C represents the mixed layer temperature variations due to the displacements of the mixed layer base, D is the air–sea heat flux storage in the mixed layer, and E is the turbulent flux at the base of the mixed layer.

Note that at the base of the mixed layer there are two contributions that can modulate the temperature of the mixed layer: Reynolds fluxes and advective or entrainment fluxes. Confusion may arise, however, since it is common to parameterize turbulent fluxes both in advective and diffusive forms. So, for example, Niiler and Kraus (1977) mixed layer models neglect friction and relate Reynolds stresses with entrainment at the mixed layer base. McPhaden (1982), on the other hand, keeps both contributions and represents the turbulent flux with an eddy diffusion term. Menkes et al. (2006) (see appendices) discuss the fact that choosing the mixed layer as we and they do in their study, causes the entrainment term to be small unless there is a barrier layer. Vincent et al. (2012) also notice that, since computation of the temperature budget is carried out in a Lagrangian framework, the contribution of vertical advection will be small but will influence the diffusive term at the mixed layer base reducing the mixed layer depth and tightening the vertical temperature gradients. Therefore, dominance of vertical shear associated mixing does not necessarily imply vertical advection and entrainment are not important.

Vertical diffusion rarely appears directly in mixed layer heat budgets and is often estimated as a residual (e.g., Du et al. 2005; Foltz et al. 2003). We explain this by the difficulty to compute this contribution in observations (because direct measurements of turbulent rate are scarce and difficult) and in models (because vertical diffusion is a highly nonlinear process which is hardly estimated offline). Here, the mixed layer heat budget is computed online to precisely evaluate this contribution as well as the other terms that appear in the equation except for the local mixed layer displacement contribution to the equation, which has to be estimated as a residual owing to time-step numerics. This is explained in the appendix of Vialard and Delecluse (1998), where one can also see that the advective terms in our heat equation include (but not separate) the horizontal and vertical advection entrainment contributions. These are caveats of our formulation but 1) the term associated with the displacement rate of mixed layer base (C) is found to be small, and 2) we verified that the horizontal entrainment of interior ocean water into sloping mixed layer is negligible compared to the dominant terms of the heat budget (as in Vialard and Delecluse 1998).

The MLD in the region varies between 20 and 60 m (Fig. 3c). We note that its spatial distribution is somewhat consistent with that of the wind stress curl (Fig. 3b), suggesting that Ekman processes are important in shaping the spatial distribution of the MLD. The dominant contributions to the mixed layer heat budget during the period June–September are the air–sea fluxes, the vertical mixing, and the advection (Fig. 4). Lateral diffusion and the term associated with the displacement rate of mixed-layer base are of secondary order and are not shown. The direct contribution of the vertical advection to the mixed layer heat budget is limited to a few grid points at the Guajira and Margarita upwelling areas (Fig. 4c). There the divergence of the surface currents at the coast brings cold waters to the
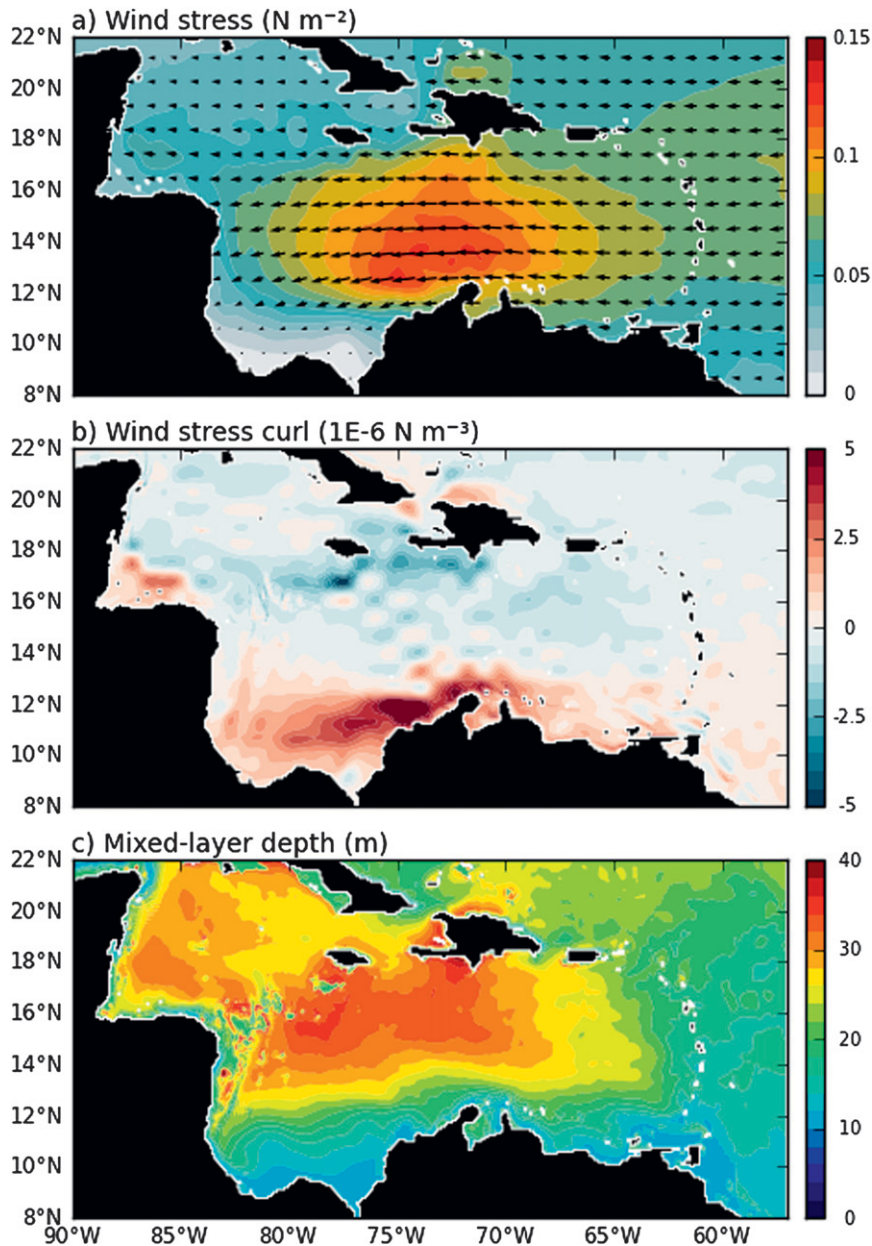
FIG. 3. Climatological average for the period June-September of (a) wind stress (N m^{-2}), (b) wind stress curl (N m^{-3}), and (c) mixed layer depth (m). The averages are built using model data from 2003 to 2009.

mixed layer. The mean meridional sections at 72°W show that upward vertical velocities at the base of the mixed layer are maximum at the coast (Figs. 5a,i). They occur in response to offshore Ekman transport at the coast (Fig. 5h). As illustrated by Fig. 5i, the upward vertical velocities either at the mixed layer base or at depth are significant only within 20 km from the coast. This distance is of same order as in Colas et al. (2011) for the Chile upwelling system or in Capet et al. (2008) for

an idealized California upwelling system. As suggested by the comparison between the Chile and Peru upwelling systems in Colas et al. (2011), such localization of the vertical velocities in a very thin band at the coast seems to be typical of upwelling systems with a sharp shelf break. Just north of the upwelling zone, downward velocity in the upper 30 m indicates that part of the waters at the coast subducts below the mixed layer (Figs. 5a,i). The cooling contribution of horizontal advection
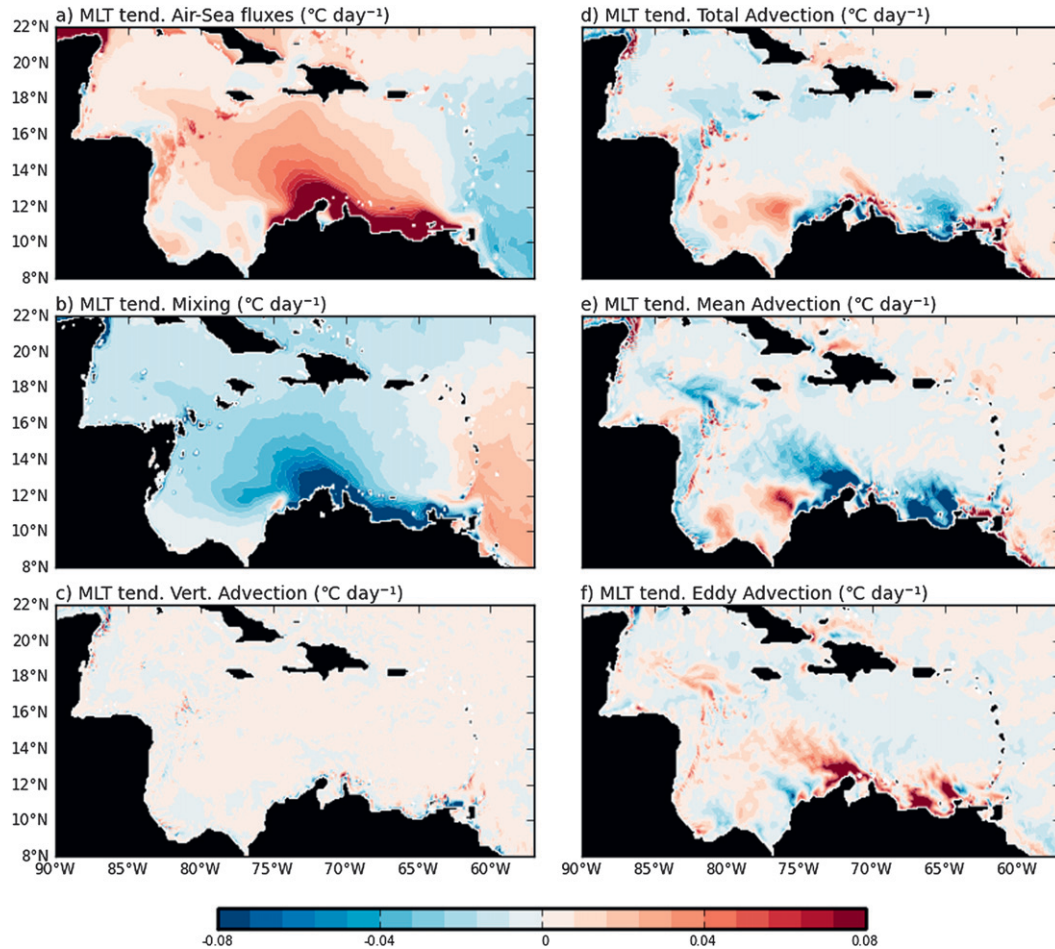
FIG. 4. Climatological average of the most important contributions to the mixed layer temperature equation (°C day^{-1}): (a) air–sea heat fluxes, (b) vertical mixing, (c) vertical advection, and (d) and total advection. The contribution of mean flow and eddies to total 3D advection of mixed layer temperature (i.e., the sum of vertical and horizontal advection) are shown in (e) and (f), respectively. The averages are built using model data from 2003 to 2009.

(Fig. 4d) is limited to a radius of 200–300 km downstream of the upwelling areas. There, the surface currents transport cold coastal waters offshore. Following Peter et al. (2006), the advection term is decomposed into mean and eddy contribution. In the mixed layer, the eddy fluxes provide a warming contribution that mostly counteracts cooling by the mean advection (Figs. 4e,f).

Vertical mixing is the dominant cooling term in the entire Caribbean (Fig. 4b). To further investigate the spatial organization of the mixing processes and their relation with 3D advection, the temperature tendency due to vertical mixing $\partial_z(K_z\partial_z T)$ and the temperature tendency due to 3D advection $u \cdot \nabla T$ are computed online at each model grid point, with K_z the vertical diffusion coefficient for tracers, $\partial_z T$ the vertical gradient of potential temperature, and **u** the 3D velocity. The corresponding turbulent heat fluxes are

computed at each depth z of the model as $Q_{zdf} = \rho_0 C_p \int_{-z}^{0} \partial_z(K_z\partial_z T)\,dz$, where ρ_0 is the water density and C_p the specific heat. We also computed the vertically integrated heat-flux divergence $Q_{adv} = \rho_0 C_p \int_{-z}^{0} u \cdot \nabla T\,dz$.

The highest contribution of vertical mixing to the mixed layer heat budget occurs along the coast (Fig. 4b). This is similar to the recent findings of Renault et al. (2012) who showed that vertical mixing is a major contributor to the surface heat budget in the Chile upwelling. Here, this maximum is explained by the high vertical shear between the shallow Caribbean Current and the subsurface Caribbean Coastal Undercurrent (Andrade et al. 2003; Jouanno et al. 2008). This is illustrated with vertical sections of zonal current and vertical shear at 72°W (Figs. 5g,d). This system is driven by the intense wind stress that occurs in the region (Fig. 3a). Close to the coast, the vertical mixing cools the surface waters
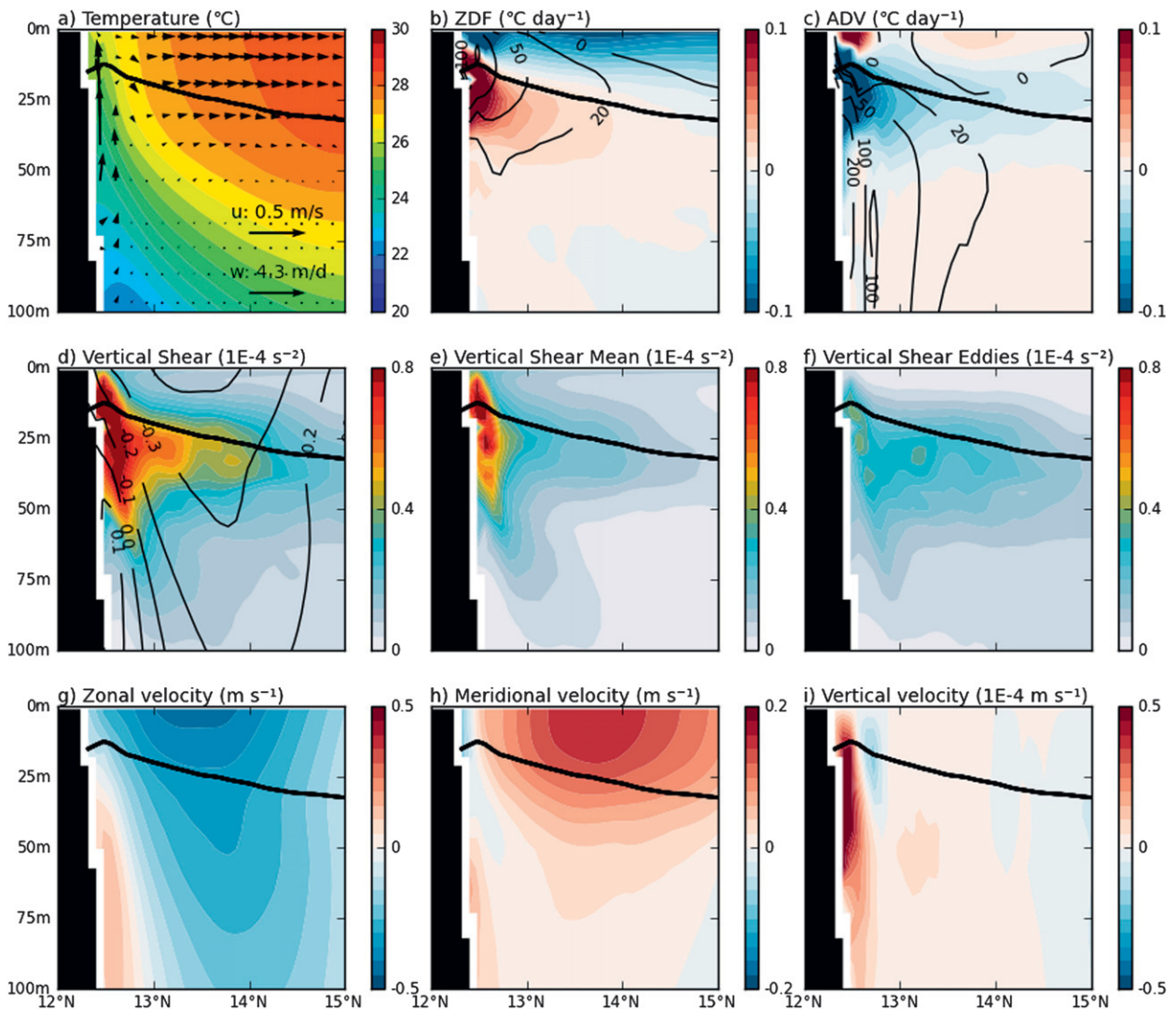
FIG. 5. Climatological meridional section at 72°W of (a) temperature (°C) and along section currents (vectors), (b) temperature tendency due to vertical mixing $\partial_z(K_z\partial_z T)$ (°C day^{-1}) and Q_{zdf} (contours of 0, 20, 50, 100, and 200 W m^{-2}), (c) temperature tendency due to 3D advection (°C day^{-1}) and Q_{adv} (contours of 0, 20, 50, 100, and 200 W m^{-2}), (d) total vertical shear $u_z^2 + v_z^2$ (10^{-4} s^{-2}) and zonal currents (m s^{-1}), (e) vertical shear (10^{-4} s^{-2}) computed from time-averaged velocity, (e) vertical shear (10^{-4} s^{-2}) computed from the corresponding velocity anomalies, (g) zonal component of the velocity (m s^{-1}), (h) meridional component of the velocity (m s^{-1}), and (i) vertical component of the velocity (10^{-4} m s^{-1}). The sum of both vertical shear contributions (e),(f) is equal to the total vertical shear shown in (d). The bold line indicates the base of the mixed layer. Computations were performed over the period June–September for years between 2003 and 2009.

and warms the subsurface waters at rates higher than 0.1°C day^{-1} (Fig. 5b). This is the signature of intense mixing between warm surface waters with cooler subsurface waters. In terms of vertical heat flux, the contribution of the vertical mixing (Q_{zdf}) reaches 200 W m^{-2} close to the coast and the surface (Fig. 5b). Significant values of Q_{zdf}, between 20 and 50 W m^{-2}, also occur at the base of the mixed layer north of 13°N. The offshore turbulent heat flux is explained by the offshore vertical shear below the mixed layer base (Fig. 5d).

The cooling contribution of the advective terms is maximum between 20 and 40 m (Fig. 5c), where the vertical mixing intensely warms the subsurface waters (Fig. 5b). This illustrates that the vertical mixing is the main process that brings the cool waters to the surface while the main role of advection is to provide or to renew the subsurface cold waters. At the coast, the contribution from advection to the vertical heat flux (Q_{adv}) also reaches 200 W m^{-2} at depths below 40 m. At other latitudes, the maxima of Q_{adv} and Q_{zdf} are of the same
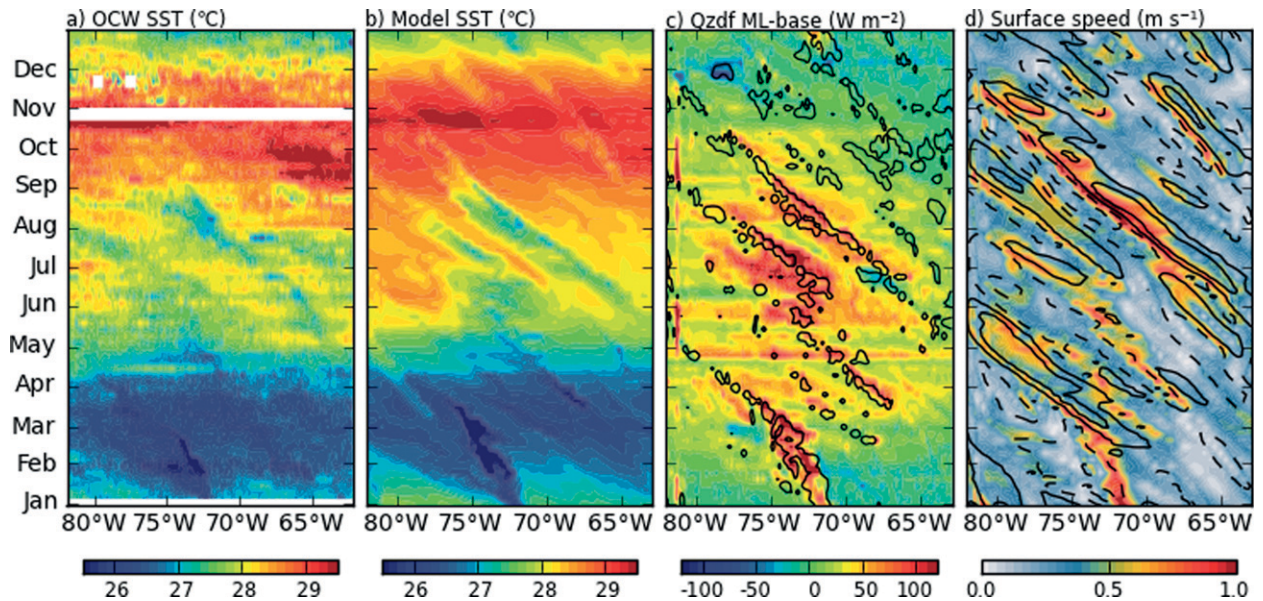
FIG. 6. Longitude–time diagrams at 14°N during year 2006 of (a) observed SST (°C), (b) model SST (°C), (c) Q_{zdf} at the mixed layer base (colors, W m^{-2}) and contours of vertical shear at 30 m depth (5×10^{-5} s^{-2}), and (d) surface speed (m s^{-1}) and contours of sea level height anomaly (-15, -5, 5, and 15 cm; dashed is negative).

order (between 20 and 50 W m^{-2}). This illustrates that the intensities of subsurface heat divergence and near-surface turbulent heat fluxes are highly interdependent. On the one hand, strong vertical mixing produces intense subsurface temperature gradients that lead to high values of Q_{adv}. On the other, near-surface Q_{zdf} is strong because cold waters are brought or renewed at the subsurface so that vertical gradients of temperature are maintained.

The origin of the band of high vertical shear below the mixed layer can be inferred through decomposition of the total shear (Fig. 5d) into mean and eddy contributions: $U_z^2 + V_z^2$ and $u_z'^2 + v_z'^2$, with (U, V) the climatological June–September mean velocity and (u', v') the corresponding velocity anomalies. At the coast, the mean flow is mostly responsible for the shear that occurs below the mixed layer (Fig. 5e), but north of 13°N about half of the vertical shear is due to velocity anomalies (Fig. 5f). This suggests that eddies play a significant role in the control of the vertical mixing offshore.

The high nonlinearity of the vertical diffusion term does not allow for properly separating the contribution of the mean flow from that of the eddies as is done with the advective terms. Nevertheless a qualitative understanding can be reached when looking at selected events. Longitude–time diagrams of observed and model SST at 14°N are shown for year 2006 (Figs. 6a,b). In both datasets the most characteristic feature is the presence of westward-propagating SST anomalies. They occur

mainly during the onset phase of the AWP (May–August) and during boreal winter when the SSTs are at their minimum. The strongest anomalies are seen between 70° and 75°W and may shape the SST seasonal cycle in this region. They are associated with high Q_{zdf} at the mixed layer base (>100 W m^{-2}) and increased vertical shear at 40 m (Fig. 6c), suggesting that subsurface turbulent heat fluxes contribute to the maintenance of the SSTs anomalies. The propagation speed of these SST anomalies is about 14 cm s^{-1}. This value is consistent with estimates of translation speeds for Caribbean anticyclones (13.5 cm s^{-1}; Richardson 2005).

High vertical shear occurs where the surface currents are maximum (Fig. 6d), generally on the downstream side of large anticylones (identified by positive sea level anomalies in Fig. 6d). A snapshot of model outputs on 28 August 2006 further illustrates this aspect (Fig. 7). The large eddy north of the Guajira Peninsula presents a strong asymmetry. Maximum velocities occur on the western side of the eddy (Fig. 7b) and are confined to the upper 50 m (Fig. 7g). Such asymmetry may arise from the deformation of the mesoscale field. Indeed, the mesoscale strain

$$\alpha = \sqrt{(u_x - v_y)^2 + (v_x + u_y)^2}$$

is maximum on the downstream side of the eddy (Fig. 7e) and in the upper ocean (Fig. 7j). The intensified surface
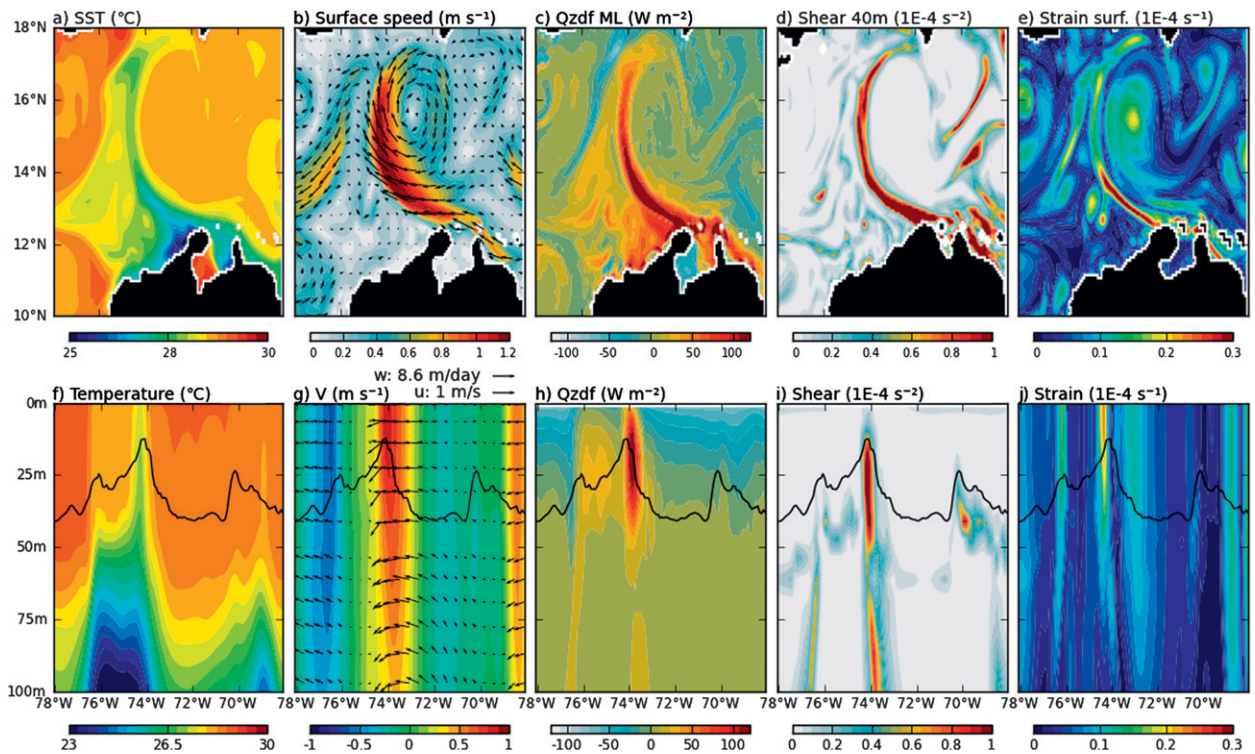
FIG. 7. Model snapshots on 28 Aug 2006. Horizontal fields of (a) surface temperature (°C), (b) speed of the surface currents (m s^{-1}), (c) Q_{zdf} at the mixed-layer base (W m^{-2}), (d) vertical shear at 40 m depth (10^{-4} s^{-2}), and (e) strain α at the surface (10^{-4} s^{-2}). Corresponding vertical sections at 14°N of (f) temperature (°C), (g) meridional currents (m s^{-1}) and (u, w) current vectors, (h) turbulent heat flux Q_{zdf} (W m^{-2}), (i) vertical shear (10^{-4} s^{-2}), and (j) strain α (10^{-4} s^{-2}).

currents increase the vertical shear (Figs. 7d,i). This results in turbulent heat flux reaching 100 W m^{-2} at the base of the mixed layer. (Figs. 7c,h). This subsurface heat flux is probably the main process responsible for the maintenance of mesoscale plumes of cool waters seen in the model (Fig. 7a) or observations (Fig. 1). Interestingly, Q_{zdf} is negative near 76°W (Figs. 7c,h). This could be the signature of convective processes at the plume front, which arise from static instability between surface cold waters advected westward and warmer waters in subsurface.

4. Discussion and summary

Mixed layer diagnostics show that vertical mixing is a key factor for the control of the SST in the Caribbean Sea during the onset of the AWP, while significant time-averaged contribution of advection is limited to 300 km around the coastal upwelling areas. The role played by the mixing in the region was already suggested by Lee et al. (2007) but not demonstrated.

The results presented in this study go against the conventional view that offshore cold water signature in the region is due to the direct effect of surface layer

Ekman transport away from the coast. First, the negative vertical velocity in Fig. 5i north of the upwelling area indicates that subduction processes occur at the Guajira upwelling, so all the waters brought to the surface at the coast are not expected to remain at the surface. This is in agreement with Capet et al. (2008) who suggest that a substantial fraction of newly upwelled water is subducted on its way seaward. Second, this conventional view does not take into account the role of the alongshore coastal current system formed by a surface current and a subsurface countercurrent, which is an important source of mixing and mixed layer turbulent cooling. Such coastal current structure as observed at the Guajira upwelling appears to be ubiquitous in most of the upwelling systems (e.g., Marchesiello et al. 2003; Colas et al. 2011). The importance of vertical mixing as a mechanism of control for the surface cooling, as highlighted by our study, is in agreement with findings in the Chile upwelling system by Renault et al. (2012). From comparison between two simulations, these authors found that the weakening of coastal winds in the dropoff zone has a larger effect on vertical mixing than on vertical advection, with both effects contributing to a reduction of cooling.

So the computation of upwelling indexes based on offshore Ekman transport may miss important processes and one can question the reliability of such quantity for the Caribbean upwelling. Our guess is that offshore Ekman transport remains a valuable first-order estimate of surface cooling in the Caribbean, not only because this process directly brings waters to the surface and near-surface but also because it controls the strength of the alongshore current system and in this way the vertical mixing and associated turbulent heat fluxes. Although our diagnostics suggest that the vertical mixing is the main contributor to the mixed layer cooling at the coast, note that we do not claim that vertical advection does not matter in the upwelling process. If cold water would not be brought by the vertical advection to the subsurface, the mixing would not be as efficient to cool the surface. And inversely, without vertical mixing (or any other transformation process) a large part of the upwelled waters would sink. The interplay between these processes in the near shore clearly requires further investigations.

As illustrated in Jouanno et al. (2012) for the Caribbean upwelling system, the semiannual cycle of the westward CLLJ forces semiannual cycles of surface coastal current north of the Guajira Peninsula and vertical shear in the southern basin. This variability is in agreement with the semiannual surface cooling observed between 80° and 70°W at the coast with peaks in January–March and June–August (Fig. 2c). The strengthening of the surface current is associated with seasonal coastal depressions of the sea level (Jouanno et al. 2012), suggesting 1) that the surface coastal current is in geostrophic balance and 2) that anomalous offshore Ekman drift in response to intensified alongshore CLLJ winds is the main driver of the coastal current acceleration.

Large mesoscale eddies are found to contribute to SST cooling through modulation of the vertical mixing by the intense jets that form on the downstream front of the eddies. These mixed-layer jets may arise from the deformation of the mesoscale field but we could not determine whether this asymmetry is caused by the local wind, the presence of the coast, or the interaction with the mean flow. Further process studies are required to elucidate this aspect.

Several studies have shown a dependence of the upwelling to the wind profile at the coast (e.g., Capet et al. 2004; Renault et al. 2012). The wind product used here allowed to adequately simulate the spatial and seasonal variability of the Caribbean upwelling and mesoscale fields. For this reason, we did not investigate further the sensitivity to higher-resolution wind products but it would be an interesting subject to in another study.

Colas et al. (2011) found that the offshore Ekman flux alone cannot explain the oceanic cooling in the 500 km off the coast of Peru. Instead they suggest that the combination of mean and eddy fluxes is necessary to sustain the offshore oceanic cooling. They suggest that this offshore cooling occurs in the subsurface but that episodic vertical mixing provides the connection with the surface. But they did not provide further details on the mechanisms driving this vertical mixing. In the Caribbean Sea, our results suggest that the intensity of the offshore vertical mixing is a factor probably as important as the lateral exchange of mass (either at the surface or subsurface) for the control of the offshore oceanic cooling. It would be interesting to estimate whether such mechanisms are at play in subtropical eastern boundary upwelling systems, where mesoscale eddies are ubiquitous.

REFERENCES

Andrade, C. A., and E. D. Barton, 2005: The Guajira upwelling system. *Cont. Shelf Res.,* **25,** 1003–1022.

——, ——, and C. N. K. Mooers, 2003: Evidence for an eastward flow along the Central and South American Caribbean Coast. *J. Geophys. Res.,* **108,** 3185, doi:10.1029/2002JC001549.

Barnier, B., and Coauthors, 2006: Impact of partial steps and momentum advection schemes in a global ocean circulation model at eddy-permitting resolution. *Ocean Dyn.,* **56** (5–6), 543–567.

Blanke, B., and P. Delecluse, 1993: Variability of the tropical Atlantic Ocean simulated by a general circulation model with two different mixed layer physics. *J. Phys. Oceanogr.,* **23,** 1363–1388.

Capet, X. J., P. Marchesiello, and J. C. McWilliams, 2004: Upwelling response to coastal wind profiles. *Geophys. Res. Lett.,* **31,** L13311, doi:10.1029/2004GL020123.

——, F. Colas, J. C. McWilliams, P. Penven, and P. Marchesiello, 2008: Eddies in eastern boundary subtropical upwelling systems. *Ocean Modeling in an Eddying Regime, Geophys. Monogr.,* Vol. 177, Amer. Geophys. Union, 131–147.

Colas, F., J. C. McWilliams, X. Capet, and J. Kurian, 2011: Heat balance and eddies in the Peru–Chile current system. *Climate Dyn.,* **39,** 509–529, doi:10.1007/s00382-011-1170-6.

Du, Y., T. Qu, G. Meyers, Y. Masumoto, and H. Sasaki, 2005: Seasonal heat budget in the mixed layer of the southeastern

tropical Indian Ocean in a high-resolution ocean general cir-
culation model. *J. Geophys. Res.,* **110,** C04012, doi:10.1029/
2004JC002845.

Foltz, G. R., S. A. Grodsky, J. A. Carton, and M. J. McPhaden,
2003: Seasonal mixed layer heat budget of the tropical
Atlantic Ocean. *J. Geophys. Res.,* **108,** 3146, doi:10.1029/
2002JC001584.

Inoue, M., I. C. Handoh, and G. R. Bigg, 2002: Bimodal distribu-
tion of tropical cyclogenesis in the Caribbean: Characteristics
and environmental factors. *J. Climate,* **15,** 2897–2905.

Jouanno, J., J. Sheinbaum, B. Barnier, J.-M. Molines, L. Debreu,
and F. Lemarié, 2008: The mesoscale variability in the Ca-
ribbean Sea. Part I: Simulations and characteristics with an
embedded model. *Ocean Modell.,* **23,** 82–101, doi:10.1016/
j.ocemod.2008.04.002.

——, ——, ——, ——, and J. Candela, 2012: Seasonal and in-
terannual modulation of the eddy kinetic energy in the Ca-
ribbean Sea. *J. Phys. Oceanogr.,* **42,** 2041–2055.

Large, W. L., and S. G. Yeager, 2004: Diurnal to decadal global
forcing for ocean and sea-ice models: The data sets and flux
climatologies. NCAR Tech. Rep. TN-460+STR, 105 pp.

Lee, S.-K., D. B. Enfield, and C. Wang, 2007: What drives seasonal
onset and decay of the Western Hemisphere warm pool?
J. Climate, **20,** 2133–2146.

Madec, G., 2008: ''NEMO ocean engine.'' Institut Pierre-Simon
Laplace Nôte du Pole de Modélisation No. 27, 367 pp.

Marchesiello, P., J. C. McWilliams, and A. Shchepetkin, 2003:
Equilibrium structure and dynamics of the California Current
System. *J. Phys. Oceanogr.,* **33,** 753–783.

McPhaden, M. J., 1982: Variability in the central equatorial Indian
Ocean. Part II: Oceanic heat and turbulent energy balance.
J. Mar. Res., **40,** 403–419.

Menkes, C. E. R., J. Vialard, S. C. Kennan, J. Boulanger, and
G. Madec, 2006: A modeling study of the impact of tropical
instability waves on the heat budget of the eastern equatorial
Pacific. *J. Phys. Oceanogr.,* **36,** 847–865.

Niiler, P. P., and E. B. Kraus, 1977: One dimensional models of the
upper ocean. *Modeling and Prediction of the Upper Layers of
the Ocean,* E. B. Kraus, Ed., Pergamon Press, 143–172.

Peter, A.-C., M. Le Hénaff, Y. Du Penhoat, C. E. Menkes, F. Marin,
J. Vialard, G. Caniaux, and A. Lazar, 2006: A model study of the
seasonal mixed-layer heat budget in the equatorial Atlantic.
J. Geophys. Res., **111,** C06014, doi:10.1029/2005JC003157.

Renault, L., and Coauthors, 2012: Upwelling response to atmo-
spheric coastal jets off central Chile: A modeling study of
the October 2000 event. *J. Geophys. Res.,* **117,** C02030,
doi:10.1029/2011JC007446.

Richardson, P., 2005: Caribbean Current and eddies as observed by
surface drifters. *Deep-Sea Res. II,* **52,** 429–463.

Tréguier, A., and Coauthors, 2001: An eddy permitting model of
the Atlantic circulation: Evaluating open boundary condi-
tions. *J. Geophys. Res.,* **106** (C10), 22 115–22 130.

Vialard, J., and P. Delecluse, 1998: An OGCM study for the TOGA
decade. Part I: Role of salinity in the physics of the western
Pacific fresh pool. *J. Phys. Oceanogr.,* **28,** 1071–1088.

Vincent, E. M., M. Lengaigne, G. Madec, J. Vialard, G. Samson, N. C.
Jourdain, C. E. Menkes, and S. Jullien, 2012: Processes setting the
characteristics of sea surface cooling induced by tropical cy-
clones. *J. Geophys. Res.,* **117,** C02020, doi:10.1029/2011JC007396.

Wang, C., 2007: Variability of the Caribbean low-level jet and its
relations to climate. *Climate Dyn.,* **29,** 411–422.

——, D. B. Enfield, S.-K. Lee, and C. W. Landsea, 2006: Influences
of Atlantic warm pool on Western Hemisphere summer
rainfall and Atlantic hurricanes. *J. Climate,* **19,** 3011–3028.